Soft Matter

Accepted Manuscript

ROYAL SOCIETY OF CHEMISTRY

www.rsc.org/softmatter

Residence-time dependent cell wall deformation of different *Staphylococcus aureus* strains on gold measured using surface-enhanced-fluorescence

Jiuyi Li,[ab] Henk J. Busscher,[a] Jan J. T. M. Swartjes,[a] Yun Chen,[a] Akshay K. Harapanahalli,[a] Willem Norde,[a] Henny C. van der Mei,[a] Jelmer Sjollema[a*]

[a]*University of Groningen and University Medical Center Groningen, Department of Biomedical Engineering, 9713 AV Groningen, The Netherlands.*

[b]*Department of Municipal and Environmental Engineering, Beijing Jiaotong University, Beijing 100044, China.*

Corresponding author: J. Sjollema
University of Groningen and University Medical Center Groningen, Department of Biomedical Engineering, 9713 AV Groningen, The Netherlands. *E-mail: j.sjollema@umcg.nl*

Abstract

Bacterial adhesion to surfaces is accompanied by cell wall deformation that may extend to the lipid membrane with an impact on the antimicrobial susceptibility of the organisms. Nanoscale cell wall deformation upon adhesion is difficult to measure, except for *Δpbp4* mutants, deficient in peptidoglycan cross-linking. This work explores surface enhanced fluorescence to measure cell wall deformation of staphylococci adhering on gold surfaces. Adhesion-related fluorescence enhancement depends on the distance of the bacteria to the surface and the residence-time of the adhering bacteria. A model is forwarded based on the adhesion-related fluorescence enhancement of green-fluorescent microspheres, through which the distance to the surface and cell wall deformation of adhering bacteria can be calculated from their residence-time dependent adhesion-related fluorescence enhancement. The distances between adhering bacteria and a surface, including compression of their extracellular polymeric substance (EPS)-layer, decrease up to 60 min after adhesion, followed by cell wall deformation. Cell wall deformation is independent on the integrity of the EPS-layer and proceeds fastest for a *Δpbp4* strain.

Introduction

Bacterial adhesion to substratum surfaces constitutes the first step in the formation of a biofilm. Biofilms can pose considerable problems in many industrial and environmental applications and over 60% of all human bacterial infections are due to biofilms.[1,2] On the other hand, there are applications where the development of biofilms is beneficiary to processes like bioremediation of soil, or to support host-protection against invading pathogens.[3,4] The bacterial cell wall consists of a relatively soft outermost layer, crucial for adhesion and biofilm formation, and a more rigid, hard core enveloped by a cross-linked peptidoglycan layer. The peptidoglycan layer is relatively thick in Gram-positive bacteria as compared to Gram-negative ones. The outermost bacterial cell layer can be composed of a variety of different surface appendages and a matrix of "extracellular polymeric substances" (EPS) containing amongst others, polysaccharides, lipids, proteins and eDNA.[2,5,6] eDNA is pivotal for the integrity of the EPS-layer around a bacterium and serves as a glue holding its various components together.[7-9]

The outermost surface of bacteria behaves differently upon adhesion to a substratum surface than the one of inert, non-biological particles, although similarities exist too. Both adhering bacteria as well as inert particles show initial maturation of the adhesive bond by progressive removal of interfacial water, re-arrangement of surface structures to increase the number of contact points and structural adaptation of surface-associated macromolecules. Residence-time dependent desorption phenomena in a parallel plate flow chamber, time dependent adhesion force measurements using atomic force microscopy (AFM) and experiments with a quartz-crystal microbalance with dissipation (QCM-D) have all indicated that this type of physico-chemical bond-maturation proceeds on a time-scale of up to several minutes.[10] The forces involved in bacterial adhesion to a substratum surface not only affect this initial bond-maturation, but moreover dictate the amount of EPS produced[11] and, when exceeding a threshold force, lead to so-called "stress de-

activation" of an adhering bacterium.[12] Stress de-activation can become so severe as to cause cell death. Nanoscale cell wall deformation upon bacterial adhesion to a substratum surface has been suggested to trigger the bacterial response to an adhering state.[13,14] Nanoscale bacterial cell wall deformation is extremely difficult to measure due to the rigidity of the peptidoglycan layer. The little evidence available for bacterial cell wall deformation as a result of adhesion to a surface, stems from work with so-called *Δpbp4* isogenic mutants. *Staphylococcus aureus Δpbp4* mutants lack chemical cross-linking in their peptidoglycan layers,[3] and accordingly relatively large deformations of up to 100-300 nm have been reported, depending upon the method applied.[15] Thus by extrapolation, it can be expected that wild-type strains with cross-linked peptidoglycan also deform as a result of their adhesion to a surface, but less than their *Δpbp4* isogenic mutants.

Surface enhanced fluorescence (SEF) is a relatively newly discovered phenomenon that was first described for fluorescent proteins and later also for fluorescently-engineered bacteria. It involves enhanced emission of fluorescent light when fluorophores come close to a reflecting metal surface, a mechanism which has been widely investigated during the last 10 years.[16-19] SEF on average extends over a distance of around 30 nm and decreases exponentially with separation distance between the fluorophore and the reflecting surface, as demonstrated by measuring SEF of proteins adsorbed to reflecting surfaces with polymeric spacers of different lengths in between.[20,21] In principle, bacterial cell wall deformation brings the intracellular content closer to a substratum surface, and hence it can be expected that SEF will enable quantitative evaluation of cell wall deformation of fluorescent bacteria upon their adhesion to a reflecting substratum.

The aim of this study is to measure SEF of three green-fluorescent *S. aureus* strains upon adhesion to gold surfaces as a function of their residence-time. Secondly, a model is proposed to describe the decrease of SEF with distance between green-fluorescent microspheres and a reflecting gold surface, based on the measurement of SEF of green-

fluorescent microspheres adhering to gold-coated quartz surfaces with adsorbed poly(ethylene glycol) methyl ether thiol (PEG-thiols) layers of different thickness. Further elaboration of the model enables to quantitatively evaluate bacterial cell wall deformation from SEF. Two *S. aureus* strains with different expression of EPS were employed, as well as a *Δpbp4* mutant, expected to yield more extensive cell wall deformation than its parent strain. All strains were evaluated prior to and after treatment with DNase I to disrupt the integrity of their EPS,[22] therewith enabling to distinguish between effects of initial deposition, compression of EPS, and cell wall deformation. *S. aureus* was chosen as it represents a major pathogen in human health and disease, with especially pathogenic traits when involved in biomaterial-associated infections.

Experimental details

Bacterial strains and cultures

Three different *S. aureus* strains were involved in this study, *i.e. S. aureus* RN4220, *S. aureus* ATCC 12600 and its isogenic *Δpbp4* mutant differing in the degree of cross-linking of their peptidoglycan layer.[3] To generate GFP expressing bacteria, the plasmid pMV158 GFP containing optimized GFP under control of the constitutively expressed MalP promotor,[23] was introduced into these *S. aureus* strains by electroporation.[24] Bacteria were routinely cultured aerobically at 37°C on a Tryptone Soya Broth (TSB; OXOID, Basingstoke, England) agar plate supplemented with 10 μg mL^{-1} tetracycline. One colony was used to inoculate 10 mL TSB also supplemented with 10 μg mL^{-1} tetracycline and this pre-culture was grown for 24 h at 37°C. The pre-culture was diluted 1:20 in 200 mL TSB and grown for 16 h at 37°C. Cultures were harvested by centrifugation (Beckman J2-MC centrifuge, Beckman Coulter, Inc., CA, USA) for 5 min at 4000 g, and washed twice with

10 mL phosphate buffered saline (PBS: 5 mM K_2HPO_4, 5 mM KH_2PO_4, 0.15 M NaCl, pH 7.0). To break staphylococcal aggregates, sonication at 30 W (Vibra Cell Model 375, Sonics and Materials Inc., Danbury, CT, USA) was applied (3 times 10 s), while cooling in an ice/water bath. Finally, bacteria were resuspended in PBS to a concentration of 3×10^8 mL^{-1} as determined in a Bürker-Türk counting chamber. The hydrodynamic diameter of these staphylococci amounted 1.2 μm on average, as determined using dynamic light scattering.

DNase I treatment

All three *S. aureus* strains produced EPS, as they grew black colonies on Congo Red agar plates (data not shown). To address the contribution of the EPS-matrix on cell wall deformation, bacterial pellets harvested from 200 mL TSB culture were suspended in 10 mL PBS solution with 100 μg mL^{-1} DNase I (Fermentas Life Sciences, Roosendaal, The Netherlands) for 1 h at 37°C, after which sonication at 30 W was applied (3 times 10 s) to remove naturally present endogenous eDNA and therewith disrupting the EPS-matrix on the bacterial cell surfaces and slightly reducing the staphylococcal diameter to 1.1 μm. Subsequently, bacteria were harvested, washed and sonicated to break staphylococcal aggregates, as described above. Finally, bacteria were resuspended in PBS to a concentration of 3×10^8 mL^{-1}, also as described above.

Fluorescent microspheres

Green-fluorescent polystyrene microspheres with a size similar to the one of staphylococci, *i.e.* with a similar diameter as the staphylococci of 1.1 μm (Molecular Probes, Invitrogen Life Technology, Grand Island, NY, USA), were used to represent

undeformable fluorescent particles. Although polystyrene particles deposited from suspension can deform and coalesce upon drying to form latex films due to forces associated with the evaporation of the suspension liquid[25], polystyrene particles kept in a liquid phase will not experience such forces and can be considered undeformable. As received microsphere suspensions were diluted in PBS to a concentration of 1×10^7 mL^{-1} as determined in a Bürker-Türk counting chamber.

Gold-coated surfaces, coupling of PEG-thiols and their layer thickness using QCM-D

Gold-coated quartz-crystal sensors (Jiaxing JingKong Electonic Co. Ltd., Jiaxing, China) were used as a reflecting substratum for staphylococcal adhesion and adhesion of green-fluorescent microspheres. Before each experiment, gold-coatings were cleaned by immersion in a 3:1:1 mixture of water, 25% $NH_3 \cdot H_2O$ and 20% H_2O_2 (Merck, Darmstadt, Germany) at 70°C for 10 min. After cleaning, gold-coated crystals were mounted in the chamber of a QCM-D (Q-Sense AB, Gothenburg, Sweden) to allow deposition of staphylococci and microspheres. The QCM-D chamber is disc-shaped with a diameter of 14 mm, and a height of 0.66 mm.

In order to establish a relation between SEF and the separation distance of fluorescent microspheres and the gold surface, gold surfaces were coated with a self-assembled monolayer of variable thickness. To this end, the gold-coated crystals were placed in the QCM-D chamber and the system was perfused with water at a flow rate of 0.144 mL min^{-1} until stable baseline values were obtained. Subsequently, the chamber was filled with a 0.2 mM PEG-thiol (molecular weight of 2000, 5000, and 10000; Sigma-Aldrich, St. Louis, MO, USA) solution in water for 30 min at room temperature after which the chamber was perfused again with water and the resulting changes in frequency and dissipation were

used to calculate the adsorbed layer thickness of the PEG-thiols with the QCM-D accompanying software package (Q-Sense, Sweden).[26]

Deposition of staphylococci and microspheres and fluorescence imaging

Next, a suspension of fluorescent staphylococci or microspheres was flown into the QCM-D chamber and flow was arrested to allow measurement of deposition using a metallurgical microscope. Since staphylococci and microspheres were suspended in relatively high ionic strength PBS, there will be no electrostatic energy barrier for deposition and deposition occurs solely under the influence of diffusion and sedimentation.[27] For deposition measurements, the microscope was equipped with a 40× objective (ULWD, CDPlan, 40PL, Olympus Co, Tokyo, Japan), connected to a CCD camera (Basler A101F, Basler AG, Germany). Staphylococci or microspheres were allowed to sediment under the influence of gravity and the number of bacteria or particles adhering per unit area was expressed as a fraction of the number of bacteria or particles adhering to the coatings in a stationary phase, *i.e.* when all staphylococci present in the chamber had deposited.

For fluorescence imaging, the entire QCM-D chamber was placed on a sample stage inside a bio-optical imaging system (IVIS Lumina II, PerkinElmer, Inc., Hopkinton, MA, USA), and the above described deposition experiments repeated. The IVIS was kept at 20°C and provided a field of view of 7.5 x 7.5 cm, to encompass the diameter of the crystal surfaces. Excitation and emission wavelengths for detection of both GFP staphylococci and microspheres were 465 nm and 515-575 nm, respectively. An exposure time of 5 s was employed and images were taken every 10 min over the entire period of 3 h. Average fluorescence radiances, R (photons s^{-1} cm^{-2} sr^{-1}) over a 1 cm^2 user-defined region of interest were determined for each image with the Living Image software package

3.1 (PerkinElmer Inc., USA) which transforms electron counts on the CCD camera to an average fluorescence radiance, taking into account the current optical parameters (area of the region of interest, magnification, binning, diaphragm, exposure time and light collecting ability of the camera as calibrated with standard light sources). The total number of staphylococci or microspheres, n_{tot}, contributing to the fluorescent radiance captured within the region of interest was around 2.0×10^7 and 6.6×10^5, respectively. Fluorescence radiance $R(t)$ was monitored as a function of time during deposition.

Calculation of residence-time dependent, adhesion-related fluorescence enhancement:

The increase of the fluorescence radiance due to adhesion of fluorescent staphylococci or microspheres was measured relative to the fluorescence of suspended ones and expressed as a total fluorescence enhancement, $TFE(t)$, according to

$$TFE(t) = \frac{R(t) - R_0}{R(0) - R_0} \qquad (1)$$

in which $R(t)$ denotes the fluorescence radiance at time t, while R_0 and $R(0)$ indicate the fluorescence radiance before and after the introduction of staphylococci or microsphere suspension into the flow chamber, respectively. $TFE(t)$ comprises the fluorescence contribution from adhering bacteria or microspheres and those still in the suspension. Fluorescence enhancement was not corrected for photobleaching, because photobleaching was found to be negligible over the time scale of the experiments (see Supporting Information, Fig. S1). Note that for staphylococci, demonstrating a residence-time dependent fluorescent enhancement, $TFE(t)$ comprises the fluorescence contribution from adhering bacteria with various residence-times and the ones still in the suspension. Accordingly,

$$TFE(t) = \frac{\varphi_0\left[\int_0^t \alpha(\tau) j(t-\tau)d\tau + \left(n_{tot} - \int_0^t j(t)dt\right)\right]}{\varphi_0 n_{tot}} \quad (2)$$

in which φ_0 is the fluorescence from staphylococci in suspension, $\alpha(\tau)$ is the adhesion-related residence-time dependent fluorescence enhancement, τ is the residence-time of adhering staphylococci, $j(t)$ is the deposition rate at time t and n_{tot} is the total number of bacteria or microspheres, both in suspension and attached, contributing to the fluorescent radiance captured within the region of interest.

In order to assess $\alpha(\tau)$, eqn (2) has been transformed to a finite summation according to

$$TFE_m = \left[\Delta t \sum_{i=1}^{m} \bar{j}_i (\alpha_{m+1-i} - 1)\right] + 1 \quad (3)$$

in which $\bar{j}_i$ is the deposition rate at time i x Δt divided by n_{tot}. Subsequently α_1, the adhesion-related fluorescence enhancement for the shortest residence-time Δt, is obtained from the first measurement after the start of an experiment at $t = \Delta t$

$$\alpha_1 = \frac{TFE_1 - 1}{\Delta t \bar{j}_1} + 1 \quad (4)$$

In line, α_m, the adhesion-related fluorescence enhancement for residence-time m x Δt, can be calculated after m consecutive steps according to

$$\alpha_m = \frac{TFE_m + \Delta t\left[\sum_{i=1}^{m} \bar{j}_i - \sum_{i=1}^{m-1} \alpha_{m-i} \bar{j}_{i+1}\right] - 1}{\Delta t \bar{j}_1} \quad (for\ m>=2) \quad (5)$$

Statistics

Data were statistically analysed using paired, two tailed Student t-tests. Significance was established at $p < 0.05$.

Results

Fluorescence enhancement during deposition of staphylococci and microspheres

Deposition of *S. aureus* ATCC 12600^{GFP} to a gold-coated surface increased relatively fast towards a stationary level within 2 h, while its *Δpbp4*^{GFP} isogenic mutant exhibited a slightly slower increase towards stationary levels, on a comparable time-scale as of *S. aureus* RN4220^{GFP} (Fig. 1a-1c). Green-fluorescent microspheres deposited most slowly (Fig. 1d). Concurrent with increasing numbers of adhering staphylococci or microspheres, the total fluorescence enhancement increased as well, but within the time-scale of an experiment stationary levels of total fluorescence enhancement were only obtained for fluorescent microspheres and not for staphylococci. Treatment of the staphylococci with DNase I hardly affected their deposition, while yielding a small increase in total fluorescence enhancement that is consistently present over time (see Fig. 1a-1c).

Adhesion-related fluorescence enhancement as a function of residence-time

Fluorescent enhancement will increase over time due to increasing numbers of adhering staphylococci or microspheres on the gold surface and time dependent deformation of the bacterial cell wall. Using a finite summation procedure, we were able to calculate the adhesion-related fluorescence enhancement, $\alpha(\tau)$, as a function of residence-times, τ, of adhering fluorescent bacteria and microspheres. Both bacteria as well as inert particles showed an initially high adhesion-related fluorescence enhancement (Fig. 2), followed by a continuous increase for adhering staphylococci over a time period of at least 3 h (Fig. 2a-2c) that levelled off after 1 h for *S. aureus* RN4220^{GFP} and *S. aureus* ATCC 12600^{GFP} but not for its isogenic mutant *S. aureus* ATCC 12600 *Δpbp4*^{GFP}, suggesting ongoing

deformation. For adhering fluorescent microspheres, however, a stationary level was obtained within 10 min (Fig. 2d), confirming their undeformable nature under the current experimental conditions. These observations suggest that the rapid, initial increase bacterial fluorescence enhancement is due to adhesion of the staphylococci at the surface and EPS-compression, while the slower, continued increase results from cell wall deformation. Importantly, the rate of continued increase is slightly higher for the *Δpbp4*^{GFP} mutant (0.11 h^{-1}) than for its parent strain (0.08 h^{-1}). Treatment of the EPS-matrix of the staphylococcal strains with DNase I consistently resulted in an increased adhesion-related fluorescence enhancement (Fig. 2a-2c).

Modelling the distance-dependence of adhesion-related fluorescence enhancement of fluorescent microspheres on PEG-thiol layers

SEF of fluorescent proteins as a function of distance has been determined on reflecting surfaces with polymeric spacers of different lengths in between.[20,21] The task at hand in this manuscript however, is more difficult and challenging, as we want to determine not only the effects of bringing an undeformed, fluorescent bacterium closer to a reflecting substratum surface as a result of deposition and EPS-compression under the influence of the adhesion forces, but we also want to quantify further deformation of the bacterial cell wall. Therefore, we first studied the time-dependence of the total fluorescence enhancement of undeformable, fluorescent microspheres adhering on gold surfaces with polymeric spacers of different molecular weights, yielding different separation distances between the microspheres and the reflecting gold surface (Fig. 3a). The thickness of the polymer layer was determined using QCM-D.

Fig. 3b presents the adhesion-related fluorescence enhancement of green-fluorescent microspheres (similarly sized as our staphylococci) on gold surfaces, coated with PEG-

thiol layers as a function of the coating thickness. Adhesion-related fluorescence enhancement for microspheres decreased with increasing thickness, *i.e.,* the separation distance between the microspheres and the reflecting gold surface. Since adhesion-related fluorescence enhancement of microspheres was immediate and not increasing over time (see Fig. 2d), it can be assumed that the surfaces of the microspheres were in direct contact with the PEG-thiol coating within the 10 min time-resolution of our measurements.

SEF of single fluorophores can be described[20,28,29] as the combined result of metal-induced increases in the rate of (1) fluorescence quenching or non-radiative decay (k_{nr}) by a factor N_{nr}, (2) fluorescence emission or radiative decay (Γ) by a factor N_r and (3) excitation of fluorophores by a factor N_{ex}. The distance-dependent adhesion-related fluorescence enhancement of a single fluorophore, $\alpha(d)$, on a reflecting metal surface can be described by the relative increase of the quantum yield $Q(d)$ as related to the quantum yield far away from the substratum, Q_∞, multiplied by the increase in the excitation rate

$$\alpha(d) = \frac{Q(d)}{Q_\infty} N_{ex}(d) \qquad (6)$$

The quantum yield, *Q(d)*, can be expressed as the ratio of radiative decay relative to the total decay,[20] *i.e.,* the sum of the radiative and non-radiative decays

$$Q(d) = \frac{N_r(d)\Gamma}{N_r(d)\Gamma + N_{nr}(d)k_{nr}} \qquad (7)$$

The rates of non-radiative and radiative decay and the excitation rates occurring in eqn (6) and (7) decrease exponentially as a function of the distance to the reflecting metal surface according to

$$N_{nr}(d) = N^0_{nr} \exp(-d/dn) + 1$$

$$N_r(d) = N^0_r \exp(-d/dr) + 1 \qquad (8)$$

$$N_{ex}(d) = N^0_{ex} \exp(-d/de) + 1$$

where *dn*, *dr*, and *de* are the characteristic distances over which these effects decrease and N^0_{nr}, N^0_r and N^0_{ex} are the non-radiative, radiative and excitation rates of single fluorophores at the surface. The distance-dependent adhesion-related fluorescence enhancement, $\alpha(d)$, of Cy3-labeled oligonucleotides on silver particles rapidly increases with their distance from the reflecting surface and amounts to around 80 at a distance of 10 nm, after which an exponential decrease sets in ranging over approximately 30 nm.[20]

In order to calculate the distance-dependent adhesion-related fluorescence enhancement, $\alpha(\delta)$ of green-fluorescent microspheres as a function of the distance, δ, between the surface of a microsphere and a reflecting gold surface, it is assumed that fluorophores distribute homogeneously within the microspheres, while we describe their volume as a stack of 100 cylindrical disks. Eqn (6) to (8) subsequently allow calculation of the fluorescent enhancement by each disk at various distances and summation values can be compared with experimental data (Fig. 3b) using a least-square fitting procedure. Note that the adhesion-related fluorescence enhancement of microspheres is maximally 1.65 at contact, which is about 50 times smaller than of fluorescent molecules. This is because for fluorescent microspheres, there is only a fraction of all fluorophores present in the region close to the reflecting surface where fluorescence enhancement is largest. In Fig. 3b it can be seen that unlike for single fluorophores, the near-linear data variation does not allow derivation of all eight model parameters occurring in eqn (6) to (8). Therefore values for the decay rates in the absence of a metal Γ (10^9 s^{-1}) and k_{nr} (4 x 10^8 s^{-1}), the enhancement

factors N^0_{nr} (38000) and N^0_r (186) and characteristic distances *dn* (8.5 Å) and *dr* (119 Å) were taken from surface enhanced fluorescence of Cy3-labeled oligonucleotides on silver particles,[20] and only values of N^0_{ex} and *de* were obtained from least-square fitting, which are the main model parameters accounting for the distance dependence of SEF. Accordingly, a high quality of the fit ($R^2 = 0.99$; see Fig. 3b) could be obtained, yielding a relation between adhesion-related fluorescence enhancement of fluorescent microspheres and their distance from a reflecting surface.

Residence-time dependent adhesion-related fluorescence enhancement and staphylococcal cell wall deformation

Adhesion-related fluorescence enhancement of undeformable fluorescent microspheres on a bare gold surface immediately reached a stationary value of around 1.6, within the time-resolution of our fluorescence measurements. Adhering staphylococci however, did not reach that level of fluorescence enhancement, which indicates that they kept a larger separation distance between the cell wall and the gold surface through the presence of the EPS-layer around them. Assuming that the GFP molecules are homogeneously distributed throughout the entire volume of the bacterial cytoplasm as enclosed by the bacterial cell wall, the separation distance can be calculated using the model for the distance-dependence of adhesion-related fluorescence enhancement forwarded above. If we assume that cell wall deformation only occurs when a bacterium has approached the gold surface to the closest possible distance, we can first derive the residence-time dependent distance between the staphylococci and the surface. The initial distance varied between 25 and 45 nm, depending on the strain considered and the distance decreased within an hour (Fig. 4). Interestingly, DNase I treated staphylococci with a disrupted EPS-layer approached the surface faster than strains with an intact EPS-layer to a distance of around 18 nm, which

we consider as the limiting distance for EPS compression. Adapting 18 nm as the closest possible distance to which bacteria can approach the substratum surface, further interpretation of adhesion-related fluorescence enhancement was done in analogy to the model outlined above for fluorescent microspheres, but now allowing cell wall deformation. Cell wall deformation brings a larger fluorescent volume of an adhering staphylococcus closer to the surface and accordingly adhering staphylococci were assumed to deform from an initial sphere with radius R_0 to an oblate ellipsoid, with a short, polar radius, b and a circular equatorial plane with radius, a. Assuming constant volume

$$V = \frac{4\pi}{3} a^2 b = \frac{4\pi}{3} R_0^3 \qquad (9)$$

The ellipsoids could also be divided in stacks of discs and using the model proposed above and the parameters presented in Fig. 3, cell wall deformation could be evaluated and expressed as the difference between the radius of the undeformed staphylococcus, R_0 and the short, polar radius of the ellipsoidally deformed bacterium. All three staphylococcal strains deformed between 1 and 3 h after deposition on the gold surface. It should be noted that deformation was calculated up to 3 h for demonstration of the principle, while under more physiologically relevant conditions adhering bacteria may well have divided by then. *S. aureus* ATCC 12600 deformed more extensively than *S. aureus* RN4220, but both strains with cross-linked peptidoglycan layers demonstrated similar cell wall deformations irrespective of DNase I treatment. *S. aureus* ATCC 12600 *Δpbp4*^{GFP}, deficient in peptidoglycan cross-linking showed the most extensive deformation of its cell wall (Fig. 4), that initially seemed dampened by the presence of an intact EPS-layer compared to the deformation observed for the DNase I treated *Δpbp4*^{GFP} mutant.

Discussion

366 The biofilm-mode of growth is a ubiquitously occurring form of bacterial growth during
367 which the organisms experience adhesion forces from the surfaces to which they adhere,
368 *i.e.* either substratum surfaces or surfaces of neighbouring bacteria. This is unlike the
369 situation during planktonic growth, where they are freely suspended in an aqueous phase.
370 The forces experienced by bacteria in a biofilm-mode of growth have been demonstrated
371 to have severe impact on their susceptibility to antimicrobials and general viability.[11,12]
372 The response of bacteria to these adhesion forces has been suggested to be due to cell wall
373 deformation, causing altered membrane stresses,[12] and re-arrangement of membrane
374 lipids.[30] AFM has demonstrated that the bacterial cell wall can indeed be deformed up to
375 the level of its rigid peptidoglycan layer, but these experiments have all been carried out
376 by wrenching bacteria between a substratum surface and an AFM-cantilever[15] or tip[31,32]
377 under the influence of an externally applied loading force, rather than under the influence
378 of the naturally-occurring adhesion force arising from a substratum surface. Besides AFM-
379 imaging of bacteria artificially immobilized on positively charged surfaces, bacterial cell
380 wall deformation under the influence of naturally-occurring adhesion forces has never
381 been demonstrated nor reliably quantified. In this study, we used recently described
382 surface enhanced fluorescence of adhering bacteria[17,24] to assess bond-maturation
383 processes and cell wall deformation of staphylococci adhering to gold surfaces.

384 To this end, we have developed a new model to describe the distance dependence of
385 SEF for undeformable fluorescent microspheres and bacteria, from which we extrapolate
386 to deformation of the rigid core of adhering bacteria containing the fluorophores. As a first
387 step in bacterial interaction with a substratum surface (see Fig. 5 for a schematic
388 summary), bacteria approach the surface and jump into contact. Jump into contact is
389 facilitated by a low energy barrier as a result of the absence of strong electrostatic
390 repulsion in PBS,[27] similar to the coalescence of two liquid layers after approach.[33] Next
391 bond-maturation processes occur, including removal of interfacial water that has been

described to occur within several minutes.[10] These initial bond-maturation processes can not be separated from effects of EPS-compression, by consequence of the 10 min time-resolution of our experiments. In initial bond-maturation, significant effects of DNase I treatment of staphylococci are seen for *S. aureus* ATCC 12600^{GFP} and *S. aureus* RN4220^{GFP}. Although initial bond-maturation is more extensive for *S. aureus* ATCC 12600^{GFP} than for its isogenic mutant *S. aureus* ATCC 12600 *Δpbp4*^{GFP} (Fig. 4), this difference disappears after DNase I treatment. *S. aureus* RN4220^{GFP} differs from *S. aureus* ATCC 12600^{GFP} in the sense that DNase I treatment of *S. aureus* ATCC 12600^{GFP} removes virtually all stainable EPS, while stainable EPS clearly remains behind after DNase I treatment in case of *S. aureus* RN4220^{GFP} (Supplementary Fig. S2). Thus, whereas DNase I treated *S. aureus* ATCC 12600^{GFP} immediately reaches the distance of closest possible approach to the gold surface, this requires more time for *S. aureus* RN4220^{GFP} (see Fig. 4). This distance of closest approach between the staphylococci adhering on a gold surface may be compared with the height of an assumed, cylindrical contact volume that can be obtained using a newly proposed elastic deformation model,[15] based on the relation between adhesion forces and externally applied, loading forces in AFM. Importantly, the elastic deformation model self-defines the height of the contact volume between adhering bacteria and substratum surfaces. In order to find confirmation for the separation of adhesion-related fluorescence enhancement into a component due to the distance between adhering bacteria and a reflecting surface and cell wall deformation, we performed AFM adhesion force measurements as a function of the external loading force and applied the above mentioned elastic deformation model (see Supplementary Fig. S3). Interestingly, regardless of the strain involved, the height of the contact cylinder was found to be around 20 nm, confirming the validity of our analysis of adhesion-related fluorescence enhancement for our strains, yielding a distance of closest approach of 18 nm.

The bacterial core of adhering staphylococci enveloped by peptidoglycan, deforms more readily in case of *S. aureus* ATCC 12600 *Δpbp4*^{GFP}, deficient in peptidoglycan cross-linking than observed for both wild-type strains, which supports the validity of our model. Nevertheless, also the staphylococcal cores enveloped by cross-linked peptidoglycan deform. DNase I treatment to disrupt the integrity of the EPS-layer, destabilizes the cell wall of the *Δpbp4*^{GFP} mutant, resulting in an almost instantaneous cell wall deformation right after adhesion. This confirms a recently proposed new role for EPS as a stress-absorber,[34] hampering cell wall deformation and the associated development of membrane stresses that may increase bacterial susceptibility to antimicrobials.[30] Cell wall deformation for *S. aureus* ATCC 12600 *Δpbp4* immobilized on a positively charged, α-poly-L-lysine coated surface, obtained using AFM-imaging and measured within approximately 1 h of contact, amounts to 49 ± 60 nm,[15] which is comparable to the deformation observed here for staphylococci after 1 h of adhesion on a negatively charged gold surface (see Fig. 4). Note that deformation observed from AFM-imaging possesses a much larger standard deviation than obtained using SEF, as SEF in essence is a macroscopic technique encompassing numbers of bacteria that exceed the numbers of bacteria involved in microscopic AFM-imaging by orders of magnitude.

The adhesion forces between the staphylococci involved in this study and the gold surfaces and responsible for the deformations as presented in Fig. 4, have been measured using AFM force measurements between staphylococci attached to a tipless cantilever and the gold coatings (see Supplementary Fig. S4). These forces initially amount around 1 nN and increase to between 2 and 3 nN after 30 s of bond-maturation under an externally applied loading force of 1 nN, regardless of the strain considered. An estimate of the deformations that might arise from these forces can be calculated using a Hertz model,[15] that considers a bacterium as a homogeneous elastic mass. Taking a Young's modulus of whole bacteria in the order of 1000 kPa,[15] it can be calculated that an adhesion force of 3

nN yields a cell wall deformation in the order of 20 - 25 nm, which is in the same range as reported here for a residence-time of adhering staphylococci of 1 h.

Wrenched between V-shaped and colloidal-probe AFM tips, deformations of Gram-negative *Pseudomonas aeruginosa* PAO1 under an externally applied force of 10 nN, exerted during a time-period of 10 s, amounted to 200 nm, while similar conditions for Gram-positive *Bacillus subtilis* 168 strain yielded 80 nm deformation.[32,35] Considering the generally short time-periods involved in these studies while yielding cell deformations in the same range as obtained here after 1 – 3 h (compare Fig. 4), it can be concluded that experiments in which bacteria are wrenched between a substratum and an AFM cantilever overestimate initial bacterial cell wall deformation. This can either be due to the fact that the externally applied forces by the AFM probe always yield a high local stress or due to the fact that it is difficult to match the externally applied force to the naturally occurring forces involved in bacterial adhesion to surfaces. Both these aspects are avoided through the use of SEF.

Conclusion

Summarizing, we have forwarded a new method to determine residence-time dependent adhesion-related fluorescence enhancement, and developed a model through which bond-maturation of bacteria adhering on reflective metal surfaces can be analyzed in terms of the distance between an adhering bacterium and the substratum, including EPS compression and cell wall deformation. Cell wall deformations arising from the measurement of adhesion-related fluorescence enhancement could be validated with AFM measurements of cell wall deformation, provided care was taken to carefully match the conditions under which the AFM experiments are carried out with the naturally occurring adhesion forces. As an important advantage of using SEF, the number of bacteria involved

in a single analysis is much larger than can be obtained using more microscopic methods, like AFM.

Cell wall deformation plays an important role in understanding bacterial susceptibility to antimicrobials as it extends to the lipid membrane and affects the lipid density in the membrane. Deformations of the bacterial cell wall as demonstrated here, are accompanied by an increase in the surface area of the lipid membrane from around 3 μm^2 to 4.5 μm^2. Therewith the distance between lipid molecules in the membrane increases, making it more susceptible for antimicrobials to penetrate. With the era of current antimicrobials approaching its end,[36] accurate measurement of cell wall deformation as a result of bacterial adhesion to surfaces, irrespective of whether of synthetic or biological origin, is thus highly important to develop alternatives for current antimicrobials.

Acknowledgements

This study was funded by the University Medical Center Groningen, Groningen, The Netherlands. JS also acknowledges financial support of Project P4.01 NANTICO of the research program of the BioMedical Materials institute, co-funded by the Ministry of Economic Affairs. JL also acknowledges support of the Fundamental Research Funds for the Central Universities 2011JBM084 in Beijing Jiaotong University, and the key project in the Chinese National Science and Technology Pillar Program during the twelve five-year plan period 2013BAJ02B02.

HJB is also director of a consulting company SASA BV. The authors declare no potential conflicts of interest with respect to authorship and/or publication of this article. Opinions and assertions contained herein are those of the authors and are not construed as necessarily representing views of the funding organizations or their respective employers.

References

1 H. J. Busscher, H. C. van der Mei, G. Subbiahdoss, P. C. Jutte, J. J. A. M. van den Dungen, S. A. J. Zaat, M. J. Schultz and D. W. Grainger, *Sci. Transl. Med.* 2012, **4**, 153rv10.

2 H. C. Flemming and J. Wingender, *Nat. Rev. Microbiol.* 2010, **8**, 623-633.

3 M. L. Atilano, P. M. Pereira, J. Yates, P. Reed, H. Veiga, M. G. Pinho and S. R. Filipe, *Proc. Natl. Acad. Sci. U. S. A.* 2010, **107**, 18991-18996.

4 G. Reid, J. A. Younes, H. C. van der Mei, G. B. Gloor, R. Knight and H. J. Busscher, *Nat. Rev. Microbiol.* 2011, **9**, 27-38.

5 G. Sheng, H. Yu and X. Li, *Biotechnol. Adv.* 2010, **28**, 882-894.

6 H. Koo, J. Xiao, M. I. Klein and J. G. Jeon, *J. Bacteriol.* 2010, **192**, 3024-3032.

7 C. Whitchurch, T. Tolker-Nielsen, P. Ragas and J. Mattick, *Science* 2002, **295**, 1487.

8 M. J. Huseby, A. C. Kruse, J. Digre, P. L. Kohler, J. A. Vocke, E. E. Mann, K. W. Bayles, G. A. Bohach, P. M. Schlievert, D. H. Ohlendorf and C. A. Earhart, *Proc. Natl. Acad. Sci. U. S. A.* 2010, **107**, 14407-14412.

9 T. Das, S. Sehar and M. Manefield, *Environ. Microbiol. Rep.* 2013, **5**, 778-786.

10 H. J. Busscher, W. Norde, P. K. Sharma and H. C. van der Mei, *Curr. Opin. Colloid Interface Sci.* 2010, **15**, 510-517.

11 H. J. Busscher and H. C. van der Mei, *PLoS Pathog.* 2012, **8**, e1002440.

12 Y. Liu, J. Strauss and T. A. Camesano, *Biomaterials* 2008, **29**, 4374-4382.

13 N. Ruiz and T. Silhavy, *Curr. Opin. Microbiol.* 2005, **8**, 122-126.

14 K. Otto and T. Silhavy, *Proc. Natl. Acad. Sci. U. S. A.* 2002, **99**, 2287-2292.

15 Y. Chen, W. Norde, H. C. van der Mei and H. J. Busscher, *Mbio* 2012, **3**, e00378-12.

16 J. Lakowicz, *Anal. Biochem.* 2001, **298**, 1-24.

17 K. Lee, L. D. Hahn, W. W. Yuen, H. Vlamakis, R. Kolter and D. J. Mooney, *Adv Mater.* 2011, **23**, H101-H104.

18 E. Le Moal, E. Fort, S. Leveque-Fort, F. P. Cordelieres, M. -P. Fontaine-Aupart and C. Ricolleau, *Biophys. J.* 2007, **92**, 2150-2161.

19 A. I. Dragan, E. S. Bishop, J. R. Casas-Finet, R. J. Strouse, J. McGivney, M. A. Schenerman and C. D. Geddes, *Plasmonics* 2012, **7**, 739-744.

20 J. Malicka, I. Gryczynski, Z. Gryczynski and J. R. Lakowicz, *Anal. Biochem.* 2003, **315**, 57-66.

21 Y. Fu and J. R. Lakowicz, *J. Phys. Chem. B.* 2006, **110**, 22557-22562.

22 M. Harmsen, M. Lappann, S. Knochel and S. Molin, *Appl. Environ. Microbiol.* 2010, **76**, 2271-2279.

23 C. Nieto and M. Espinosa, *Plasmid* 2003, **49**, 281-285.

24 J. Li, H. J. Busscher, H. C. van der Mei and J. Sjollema, *Biofouling* 2013, **29**, 11-19.

25. P. R. Sperry, B. S. Snyder, M. L. O'Dowd and P. M. Lesko, *Langmuir*, 1994, **10**, 2619-2628.

26 M. Voinova, M. Jonson and B. Kasemo, *Biosens. Bioelectron*. 2002, **17**, 835-841.

27 W. W. Wilson, M. M. Wade, S. S. Holman and F. R. Champlin, *J. Microbiol. Methods* 2001, **43**, 153-164.

28 P. Anger, P. Bharadwaj and L. Novotny, *Phys. Rev. Lett*. 2006, **96**, 113002.

29 C. Geddes and J. Lakowicz, *J. Fluoresc.* 2002, **12**, 121-129.

30 M. Isabel Perez, N. Rodriguez, J. Ocampo, J. Chavez, M. Fernanda Contreras, C. Arevalo, I. Feussner, S. Trier and C. Leidy, *Biophys. J.* 2013, **104**, 20A.

31 V. Vadillo-Rodriguez, S. R. Schooling and J. R. Dutcher, *J. Bacteriol.* 2009, **191**, 5518-5525.

32 A. V. Bolshakova, O. I. Kiselyova, I and V. Yaminsky, *Biotechnol. Prog.* 2004, **20**, 1615-1622.

33 N. Chen, T. Kuhl, R. Tadmor, Q. Lin and J. Israelachvili, *Phys. Rev. Lett.* 2004, **92**, 024501.

34 M. Crismaru, L. A. T. W. Asri, T. J. A. Loontjens, B. P. Krom, J. de Vries, H. C. van der Mei and H. J. Busscher, *Antimicrob. Agents Chemother.* 2011, **55**, 5010-5017.

35 V. Vadillo-Rodriguez, T. J. Beveridge and J. R. Dutcher, *J. Bacteriol.* 2008, **190**, 4225-4232.

36 N. Woodford and D. M. Livermore, *J. Infect.* 2009, **59**, S4-S16.

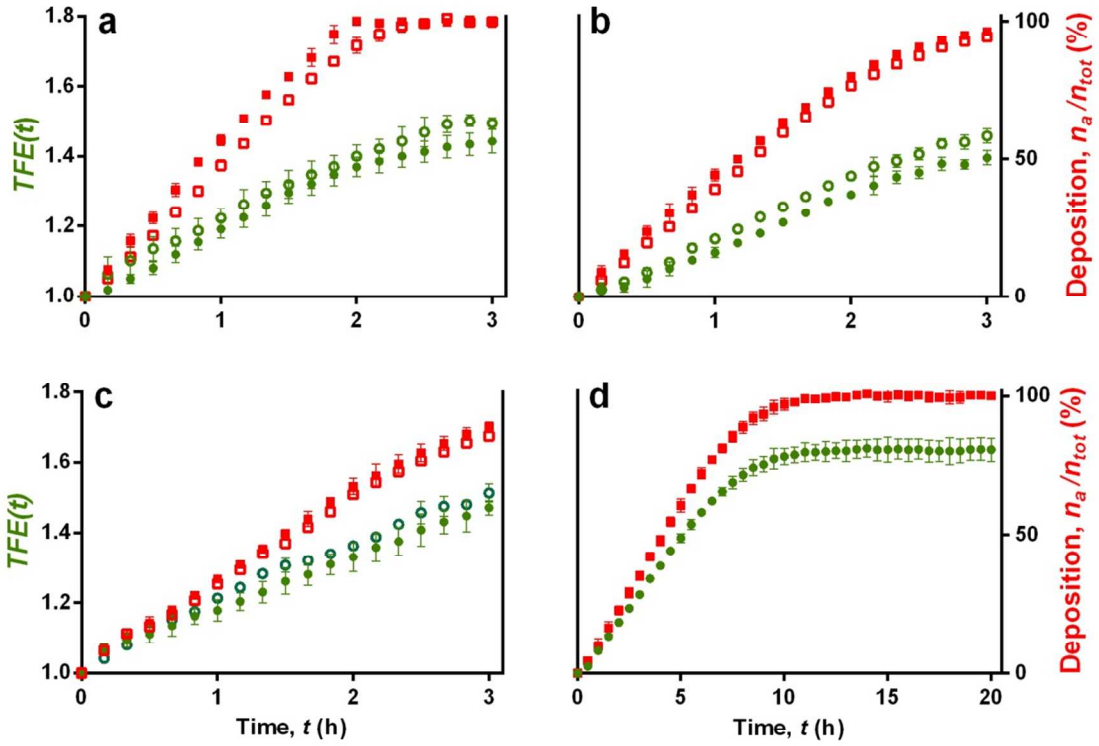

Fig. 1 Total fluorescence enhancement, TFE(t), and percentage staphylococci and microspheres deposited to a gold-coated surface as a function of deposition time for three, green-fluorescent *S. aureus* strains. (a) *S. aureus* ATCC 12600^{GFP}, (b) *S. aureus* RN4220^{GFP}, (c) *S. aureus* ATCC 12600 *Δpbp4*^{GFP} and (d) green-fluorescent microspheres (note the different time axis). TFE is due to planktonic and adhering bacteria and microspheres, while deposition is expressed as a percentage of the number of adhering bacteria or microspheres, na with respect to their total numbers in the system, n_{tot}. Error bars represent standard errors over four separate experiments with different bacterial cultures and microsphere suspensions. Open symbols represent data for staphylococci treated with DNase I.

559

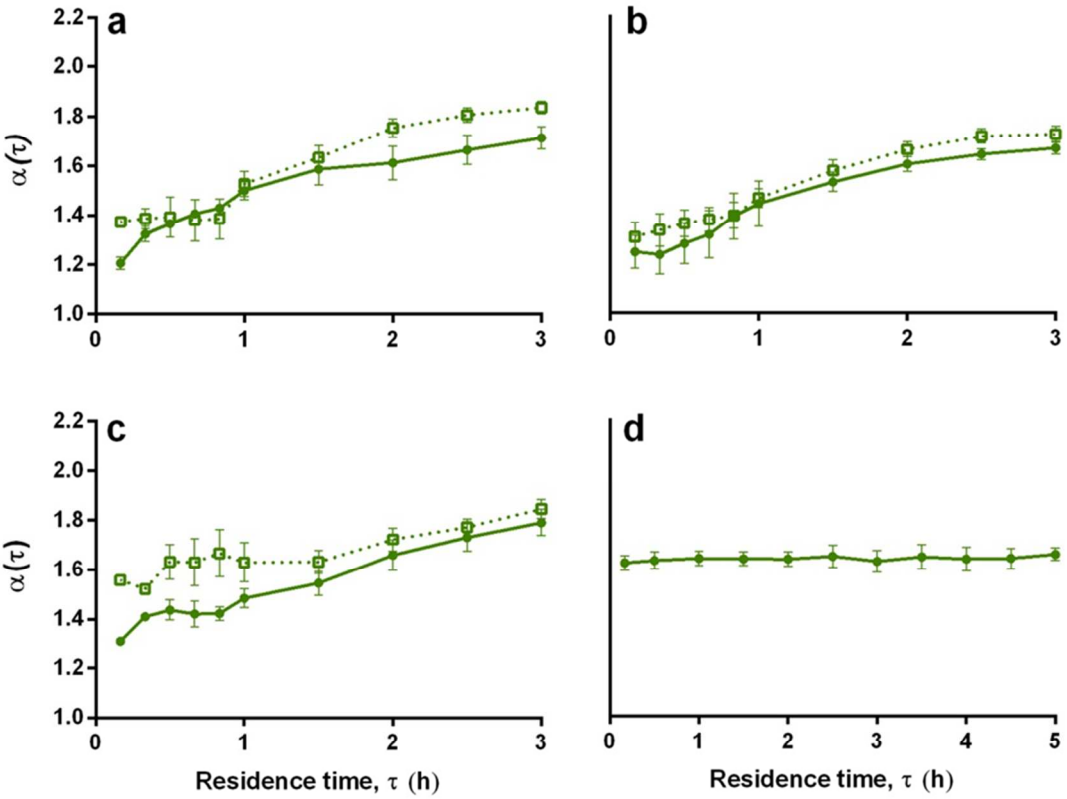

560
561 **Fig. 2** Adhesion-related fluorescence enhancement, α(τ), as a function of residence-time, τ, for three, green-
562 fluorescent *S. aureus* strains and microspheres adhering to a gold-coated surface. (a) *S. aureus* ATCC
563 12600^{GFP}, (b) *S. aureus* RN4220^{GFP}, (c) *S. aureus* ATCC 12600 *Δpbp4*^{GFP} and (d) green-fluorescent
564 microspheres. Error bars represent standard errors over four separate experiments with different bacterial
565 cultures and microsphere suspensions. Open symbols represent staphylococci treated with DNase I.

566

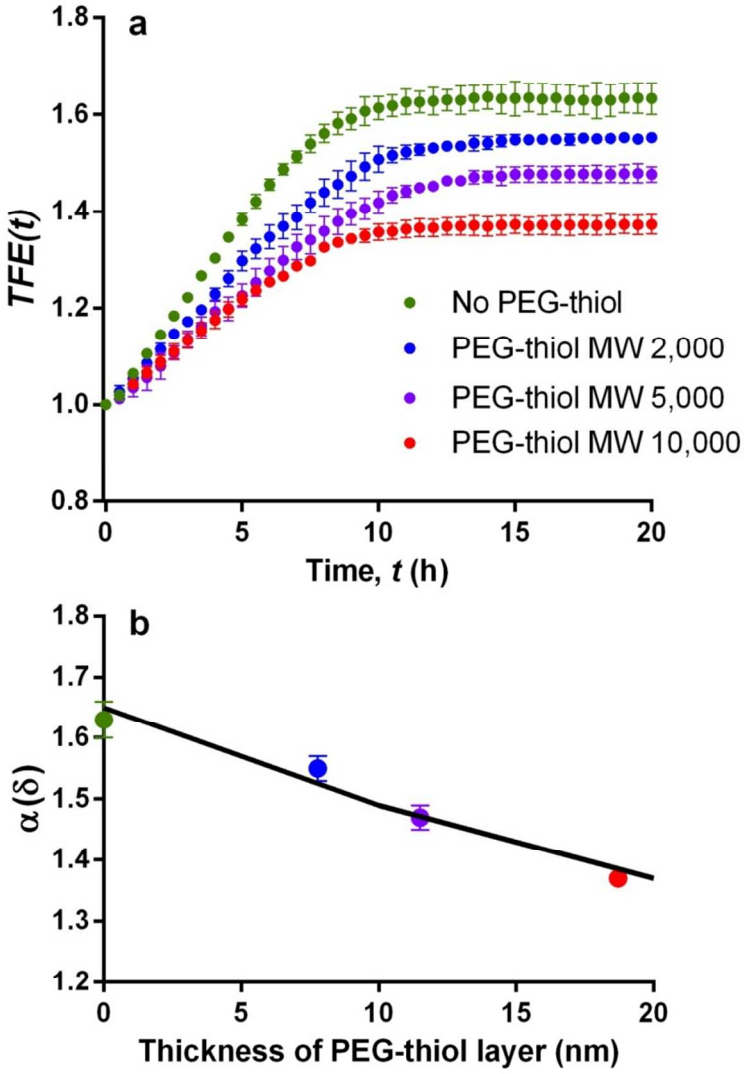

Fig. 3 Analysis of the fluorescence enhancement of green-fluorescent microspheres adhering to a gold-coated surface. (a) Total fluorescence enhancement, TFE(t) as a function of time to gold-coated surfaces with adsorbed PEG-thiol layers of different molecular weight, (b) Adhesion-related fluorescence enhancement, $\alpha(\delta)$, for green-fluorescent microspheres adhering to a gold-coated surface as a function of the adsorbed layer thickness of PEG-thiols. Fluorescent enhancement values are taken in the stationary phase of the deposition process (see Fig. 3a) and are independent of residence-time (see also Fig. 2d). Bars represent standard errors over four separate experiments with different suspensions of microspheres.

576 The solid line represents calculated adhesion-related fluorescence enhancement as a function of distance
577 according to the model presented for undeformed green-fluorescent microspheres on a reflecting metal
578 surface, using literature values for the decay rates in the absence of a metal, the enhancement factors N^0_{nr} and
579 N^0_r and the characteristic distances dn and dr.[20] The enhancement factor N^0_{ex} and characteristic distance de
580 were used as parameters in a least-square fitting procedure yielding values of 68 and 387 Å, respectively.

581

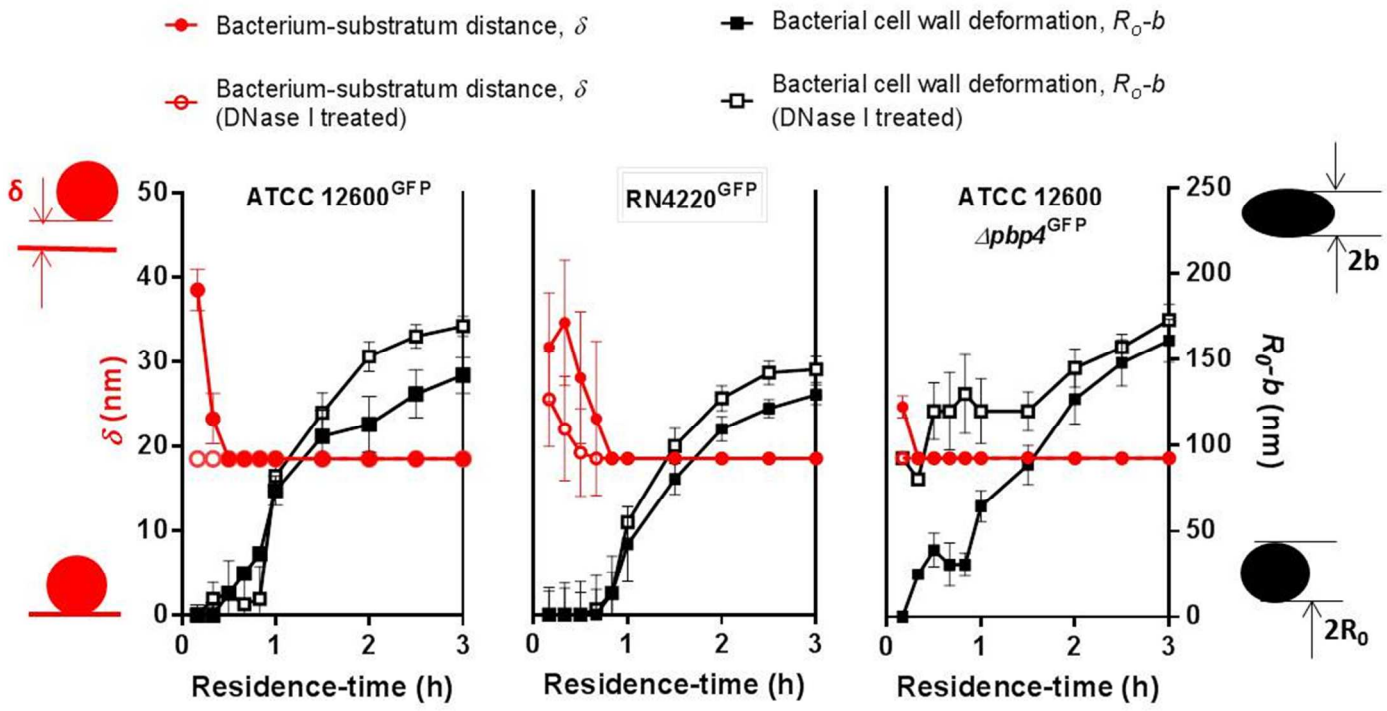

582

583 **Fig. 4** Bacterium-substratum distance, δ, and bacterial cell wall deformation, (R_0-b), as a function of the
584 residence-time of staphylococci adhering to gold surfaces. Error bars represent standard errors calculated from
585 adhesion-related fluorescence enhancement data from four different bacterial cultures.

586

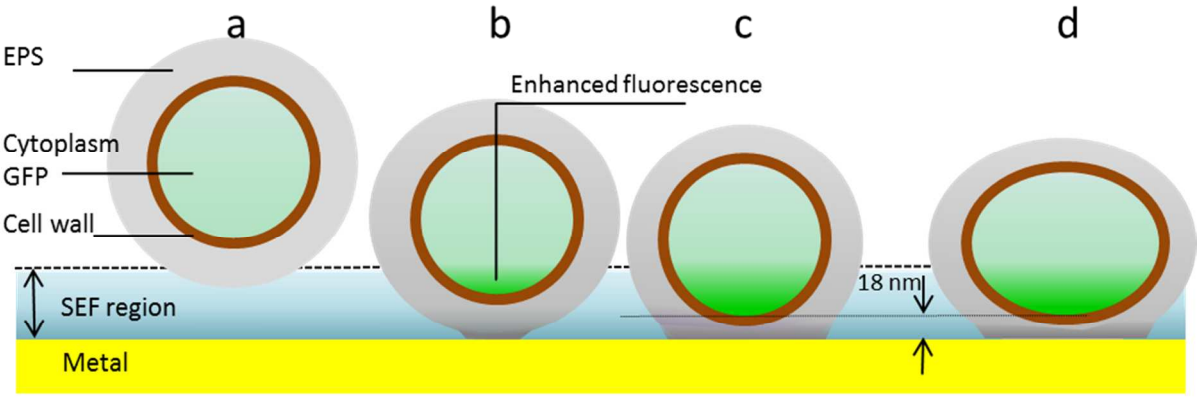

Fig. 5 Schematic presentation of the different steps in bacterial interaction with a surface and SEF events. (a) Approach of a bacterium towards the substratum surface. (b) Bacteria jump into contact and SEF occurs from the fluorophores within the cytoplasm of the bacterium, sufficiently close to the reflecting metal surface. (c) EPS is compressed under the influence of the adhesion forces between the bacterium and the substratum surfaces, bringing more fluorophores sufficiently close to the surface for SEF, up to a minimum separation distance of around 18 nm. (d) When EPS is compressed to its limiting thickness, the cell wall deforms, further increasing the number of fluorophores within the reach of SEF.